A Timer-Based Hybrid Supervisor for Robust, Chatter-Free Policy Switching

Jan de Priester, Ricardo G. Sanfelice

Keywords: Chattering, robustness, value function-based switching, hybrid control.

Summary

We address the challenge of switching among multiple learned policies in reinforcement learning control systems, where conventional value function–based methods can lead to chattering in the presence of small measurement noise. Our goal is to design a switching logic that assures asymptotic stability and maintains a robustness margin so that rapid switching is prevented under bounded measurement noise. To this end, we propose a timer-based hybrid supervisor that integrates a resettable timer that enforces a minimum dwell time on the active policy. This dwell time is adaptively adjusted by predicting the evolution of the state of the system, ensuring that a switch occurs only when a significantly better alternative is predicted. We derive sufficient conditions under which the hybrid supervisor is guaranteed to exhibit non-Zeno behavior and render a compact set robustly globally asymptotically stable in the presence of bounded measurement noise. Simulation results on representative decision-making problems demonstrate that our hybrid supervisor is robust under noisy conditions where a conventional switching strategy fails.

Contribution(s)

1. This paper presents a hybrid supervisor that maintains the asymptotic stability properties of the underlying policies and prevents chattering between the policies under bounded measurement noise. The hybrid supervisor deploys a timer-based mechanism to predict and enforce a dwell period between policy switches. Sufficient conditions are presented under which the hybrid supervisor is guaranteed to exhibit non-Zeno behavior and render a compact set robustly globally asymptotically stable in the presence of bounded measurement noise.
   Context: Chattering refers to the phenomenon of a system rapidly switching its decision due to measurement noise that results in inefficient or destabilizing behavior. Existing chattering-mitigation strategies in RL rely on partitioning the state space into overlapping regions to define switching conditions, with the overlap situated where chattering is observed. Defining these overlapping regions necessitates some insight into their expected location, making this approach more suitable when such prior knowledge is available. Alternative timer-based approaches that *may* prevent chattering impose a fixed lower bound on the time between switches. These methods are not designed to address chattering under measurement noise and thus lack formal guarantees that bounded disturbances will not induce chattering.

A Timer-Based Hybrid Supervisor for Robust, Chatter-Free Policy Switching

Jan de Priester[1], **Ricardo G. Sanfelice**[1]
{jadeprie,ricardo}@ucsc.edu

[1]**Department of Electrical and Computer Engineering, University of California Santa Cruz**

Abstract

We address the challenge of switching among multiple learned policies in reinforcement learning control systems, where conventional value function–based methods can lead to chattering in the presence of small measurement noise. Our goal is to design a switching logic that assures asymptotic stability and maintains a robustness margin so that rapid switching is prevented under bounded measurement noise. To this end, we propose a timer-based hybrid supervisor that integrates a resettable timer that enforces a minimum dwell time on the active policy. This dwell time is adaptively adjusted by predicting the evolution of the state of the system, ensuring that a switch occurs only when a significantly better alternative is predicted. We derive sufficient conditions under which the hybrid supervisor is guaranteed to exhibit non-Zeno behavior and render a compact set robustly globally asymptotically stable in the presence of bounded measurement noise. Simulation results on representative decision-making problems demonstrate that our hybrid supervisor is robust under noisy conditions where a conventional switching strategy fails.

1 Introduction

In many real-world decision-making problems, a reinforcement learning (RL) agent is faced with a choice among multiple strategies or actions, each with its own advantages and trade-offs. Such problems arise not only in control systems and robotics (Hwangbo et al., 2019), but also in areas as diverse as financial portfolio management (Bartram et al., 2021), cybersecurity (Alpcan & Baar, 2010), and video game strategy selection (Yannakakis & Togelius, 2018). In these settings, the agent must evaluate limited, often noisy information in order to select the best course of action, balancing short-term rewards against long-term objectives. This dynamic, multi-strategy decision-making process is inherently challenging, particularly in RL, where the optimal strategy may not be immediately apparent and can depend on subtle aspects of the current state or adversarial influences in the environment.

One particularly challenging phenomenon in this context is the tendency for the system to "chatter" between strategies (Prieur et al., 2007; Mayhew et al., 2011; de Priester et al., 2022; 2024). Chattering occurs when an agent rapidly switches its decision—often due to small measurement errors or environmental perturbations—resulting in inefficient or even destabilizing behavior. For example, in video game scenarios, a player or AI might oscillate between aggressive, defensive, and resource-gathering strategies in response to transient changes in the game state. Although such switching might appear adaptive in the short term, it can prevent the full exploitation of a promising strategy, ultimately leading to suboptimal performance. Furthermore, in competitive environments, adversaries can deliberately manipulate the situation to induce premature or frequent switching, thereby exploiting the hesitation or uncertainty of the decision maker (de Priester et al., 2022; 2024).

Existing chattering-mitigation strategies in RL rely on partitioning the state space into overlapping regions to define switching conditions, with the overlap situated where chattering is observed. Defining these overlapping regions necessitates some insight into their expected location, making this approach more suitable when such prior knowledge is available (de Priester et al., 2022; 2024). In contrast, our proposed method addresses scenarios where these switching regions are not easily determined. We achieve this by leveraging value function-based switching conditions, complemented by a timer-based mechanism to predict and enforce a minimum dwell period between policy switches. While there exist alternative timer-based approaches that *may* prevent chattering by imposing a fixed lower bound on the time between switches (Greene et al., 2020; Makumi et al., 2023; Chemingui et al., 2025), these methods are not designed to address chattering under measurement noise and thus lack formal guarantees that bounded disturbances will not induce chattering.

Motivated by these challenges, we propose a novel predictive timer-based hybrid supervisor that prevents chattering between policies. In Section 4, we provide a formal analysis of the proposed hybrid supervisor, establishing properties such as non-Zeno behavior and robustness to measurement noise. In Section 5, we validate our approach through numerical simulations on a representative decision-making problem.[1] Section 3 further motivates our work by presenting a detailed problem formulation and an illustrative example of the chattering issues observed with conventional switching strategies.

2 Preliminaries

2.1 Notation and Definitions

The following notation is used throughout the paper. The n-dimensional Euclidean space is denoted by $\mathbb{R}^n$; the real numbers by $\mathbb{R}$; the nonnegative reals by $\mathbb{R}_{\geq 0} := [0, \infty)$; the positive reals by $\mathbb{R}_{>0} := (0, \infty)$; the natural numbers including zero by $\mathbb{N} := \{0, 1, 2, ...\}$; and the positive natural numbers by $\mathbb{N}_{>0} := \{1, 2, ...\}$. The empty set is denoted by $\varnothing$. For a set S, $\operatorname{int}(S)$ denotes its interior and ∂S its boundary. The closed unit ball in the Euclidean norm, of appropriate dimension and centered at the origin, is denoted by $\mathbb{B}$. For a vector x and a nonempty set S, $|x|$ is its Euclidean norm, and $|x|_S := \inf_{y \in S} |x - y|$ is its distance to S. The domain of a map f is $\operatorname{dom} f$. The signum function is $\operatorname{sgn}(\chi) := -1$ if $\chi < 0$, and 1 if $\chi \geq 0$. The tangent cone to a set $S \subset \mathbb{R}^n$ at $\chi \in \mathbb{R}^n$ is $T_S(\chi)$, defined as the set of all vectors $w \in \mathbb{R}^n$ for which there exist sequences $\chi_i \in S$, $\tau_i > 0$ with $\chi_i \to \chi$, $\tau_i \searrow 0$, and $w = \lim_{i \to \infty} \frac{\chi_i - \chi}{\tau_i}$. A set-valued map F is outer semicontinuous (OSC) if for any sequence $x_i \to x$ in $\operatorname{dom} F$ with $y_i \in F(x_i)$ and $y_i \to y$, it holds that $y \in F(x)$.

2.2 Reinforcement Learning Framework

Markov decision processes (MDPs) are used as a formalism for RL (Puterman, 1994). In an MDP, the learner/controller is referred to as the agent and interacts with an environment. The state of the agent $z \in \mathcal{Z}$, where $\mathcal{Z} \subset \mathbb{R}^n$ is a set of states, evolves according to the continuous-time dynamics

$$\dot{z} = f(z, u), \tag{1}$$

where $f \colon \mathcal{Z} \times \mathcal{U} \to \mathcal{Z}$ is Lipschitz and $u \in \mathcal{U} \subset \mathbb{R}^m$ is the control input from a set of actions $\mathcal{U}$. The set of solution pairs $t \mapsto (z(t), u(t))$, where $t \in \mathbb{R}_{\geq 0}$ is the ordinary time parameter, to (1) starting from a set $X_0 \subset \mathcal{Z}$ is denoted by $\mathcal{S}(X_0)$. Given a solution pair $(z, u) \in \mathcal{S}$ to (1), the *discounted reward functional* $\mathcal{V} \colon \mathcal{S} \to \mathbb{R}$ maps solutions of (1) to the discounted reward and is defined as

$$\mathcal{V}(z, u) := \int_0^{\sup \operatorname{dom}(z,u)} e^{-\rho t} R(z(t), u(t)) \, \mathrm{d}t, \tag{2}$$

[1] All simulation files are available at https://github.com/JPriester/Timer-Value-Supervisor.

where $\rho \in \mathbb{R}_{>0}$ is the discount rate and $R\colon \mathcal{Z} \times \mathcal{U} \to \mathbb{R}$ is the reward function. The *value function* for a Lipschitz continuous policy $\pi\colon \mathcal{Z} \to \mathcal{U}$ is given by

$$V_\pi(z_0) = \mathcal{V}(z, \pi(z)) = \int_0^{\sup \operatorname{dom} z} e^{-\rho t} R(z(t), \pi(z(t)))\, \mathrm{d}t \tag{3}$$

where $(z, \pi(z)) \in \mathcal{S}(z_0)$ is the unique solution pair to the closed-loop system $\dot{z} = f(z, \pi(z))$ starting from $z_0 \in X_0$.

In this work, we apply value iteration to obtain an approximate value function $\hat{V}_\pi\colon \mathcal{Z} \to \mathbb{R}$ that approximates the true value function V_π defined in (3). We represent $\hat{V}_\pi$ using a multi-layer perceptron (MLP) with L layers and continuously differentiable activation functions, such as the sigmoid or hyperbolic tangent function. The approximate value function is given by

$$\hat{V}_\pi(z; \theta) = W_L\, h\Big(W_{L-1}\, h\Big(\cdots\, h\big(W_1 z + b_1\big) \cdots\Big) + b_{L-1}\Big) + b_L, \tag{4}$$

where $\theta = \{W_1, W_2, \ldots, W_L, b_1, b_2, \ldots, b_L\}$ denotes the collection of weights and biases, and $h\colon \mathbb{R} \to \mathbb{R}$ is a continuously differentiable activation function. For conciseness, we omit the explicit dependency on the network parameters θ in the remainder of the paper. The value iteration algorithm implemented is analogous to the training of the critic network in actor-critic methods, such as Proximal Policy Optimization (PPO) (Schulman et al., 2017).[2]

2.3 Hybrid Systems

A hybrid system $\mathcal{H} = (C, F, D, G)$ is defined as

$$\mathcal{H}: \begin{cases} \dot{x} &= F(x) \quad x \in C \\ x^+ &= G(x) \quad x \in D \end{cases} \tag{5}$$

where $x \in \mathbb{R}^n$ denotes the state variable, x^+ the state variable after a jump, $F\colon C \to \mathbb{R}^n$ is a function referred to as the flow map, $C \subset \mathbb{R}^n$ is the set of points referred to as the flow set, $G\colon D \to \mathbb{R}^n$ the jump map, and $D \subset \mathbb{R}^n$ is the jump set. When the state is in the flow set, the state is allowed to evolve continuously and is described by the differential equation defined by the flow map. When the state is in the jump set, the state is allowed to be updated using the difference equation defined by the jump map. In this way, with some abuse of notation, the solution to (5) is given by a function $(t, j) \mapsto x(t, j)$ defined on a hybrid time domain, which properly collects values of the ordinary time variable $t \in \mathbb{R}_{\geq 0}$ and of the discrete jump variable $j \in \mathbb{N}$. The hybrid system $\mathcal{H}$ allows for the combination of continuous-time behavior (flow) with discrete-time behavior (jumps). For more details on hybrid dynamical systems, see Goebel et al. (2012); Sanfelice (2021).

3 Motivation

3.1 Problem Definition

We consider systems described by the dynamics in (1). The control input to this system is provided by a continuous policy $\pi_q \in \Pi := \{\pi_1, \pi_2, \ldots, \pi_N\}$, $\pi_q\colon \mathcal{Z} \to \mathcal{U}$ selected from a policy bank Π, where each policy π_q maps states to control actions and $N \in \mathbb{N}_{>0}$ is the number of policies in the policy bank Π. Furthermore, each policy asymptotically stabilizes a compact set. A continuously differentiable approximate value function $\hat{V}_q\colon \mathcal{Z} \to \mathbb{R}$ of the form (4) is obtained for each policy $\pi_q \in \Pi$ for $q \in \mathcal{Q} := \{1, 2, \ldots, N\}$ via RL. The problem to solve is defined as follows:

Problem ($\star$) Design a value function-based switching logic that prevents chattering under measurement noise by guaranteeing a nonzero robustness margin $\varepsilon > 0$ while preserving the properties of the individual policies when they are applied to (1).

[2] For details on the implementation of the value iteration algorithm, see the GitHub link in footnote 1.

Figure 1: Left, the approximate value function $\hat{V}_1$, in blue, and $\hat{V}_2$, in green, for the policies π_1 and π_2, respectively. Right, the resulting control policy by applying the supervisory policy Q^*. The setpoints $\mathcal{Z}^*$ are denoted by the red stars.

A straightforward switching logic that selects the value of q corresponding to the highest value function $\hat{V}_q$ for the current state z, though it preserves the properties induced by the individual policies, may not be robust against measurement noise, as illustrated in the following example.

Example 1 (Stabilizing two disconnected points on a line)**.** *We consider a system evolving on a line with the state $z \in \mathcal{Z} \subset \mathbb{R}$ and dynamics $\dot{z} = u$, where $u \in [-1, 1]$ is the control input. The problem to solve consists of robustly globally asymptotically stabilizing the set $\mathcal{Z}^* := \{z_1^*, z_2^*\} := \{-1, 1\} \subset \mathcal{Z}$, which consists of two disconnected setpoints, by designing a supervisory policy to select between the two available policies, π_1 and π_2, based on the observation vector*

$$o(z+m) = \begin{bmatrix} z + m - z_1^* \\ z + m - z_2^* \end{bmatrix}, \tag{6}$$

where $m \in \mathbb{R}$ represents the measurement noise. The policies are given by

$$\pi_q(z) = z_q^* - z, \tag{7}$$

for each $z \in \mathcal{Z}$ and each value of the logic variable $q \in \{1, 2\} := \mathcal{Q}$. It can be shown that each policy in (7) globally asymptotically stabilizes one of the setpoints, namely, π_1 globally asymptotically stabilizes z_1^* and π_2 globally asymptotically stabilizes z_2^*. The value iteration algorithm is applied to find the approximate value functions $\hat{V}_q$ for $q \in \mathcal{Q}$ subject to the reward function

$$R(z) = -c_1 |z|_{\mathcal{Z}^*}, \tag{8}$$

which has a global maximum for $z = z^*$, where $c_1 \in \mathbb{R}_{>0}$ is a constant, discount rate $\rho = -\frac{1}{\Delta t} \ln 0.9$,[3] sampling time of $\Delta t = 0.05$ seconds, and a horizon of 100 time steps.

The supervisory policy $Q^* : \mathcal{Z} \to \mathcal{Q}$ that maps the state z to the logic variable q is given by

$$Q^*(z) := \{q \in \mathcal{Q} : \hat{V}_q(z) = \max_{\bar{q} \in \mathcal{Q}} \hat{V}_{\bar{q}}(z)\} \tag{9}$$

namely, the value of q corresponds to the highest approximate value function $\hat{V}_q$ for the current state z.[4] For the value function $\hat{V}_{q'}$, where $q' \in Q^*(z)$, corresponding to deploying the supervisory policy Q^*, it follows by the definition of Q^* that $\hat{V}_{q'}(z) \geq \hat{V}_q(z)$ for all $z \in \mathcal{Z}$. Figure 1 shows the approximate value function $\hat{V}_1$ and $\hat{V}_2$ for the policies π_1 and π_2, respectively, and the resulting control policy by applying the supervisory policy Q^*. Figure 1 shows that in the region $z \in [z_1^*, z_2^*]$, the supervisory policy Q^* selects the logic variable q corresponding to the closest setpoint: policy π_1 ($q = 1$) when $z \leq 0$ to stabilize z_1^*, and policy π_2 ($q = 2$) when $z > 0$ to push solutions towards z_2^*. Conversely, in the regions $z \in [-3, -1.6) \cup (1.6, 3]$, the supervisory policy Q^* opts for opposing policies: policy π_2 ($q = 2$) when $z < -1.6$, and policy π_1 ($q = 1$) when $z > 1.6$. This exploitative selection can be attributed to the opposing policies in these regions yielding a larger control input than the corresponding policies while maintaining the same sign of the control input.

[3] The chosen discount rate corresponds to a discrete-time discount factor of 0.9.

[4] For certain states, multiple maximizers may exist for the value functions in the policy bank.

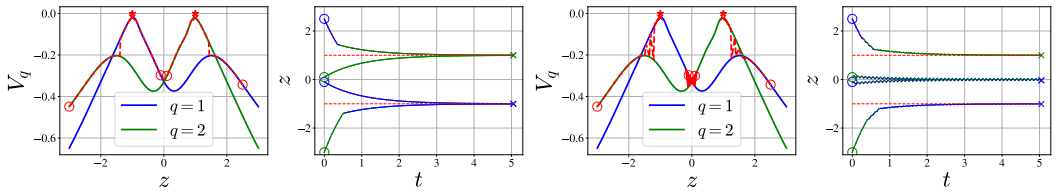

(a) Noise magnitude $\varepsilon = 0$.

(b) Noise magnitude $\varepsilon = 0.3$.

Figure 2: The solutions to the closed-loop system using the supervisory policy Q^* plotted over the approximate value function $\hat{V}_1$, in blue, and $\hat{V}_2$, in green, for the policies π_1 and π_2, respectively, and over time under the measurement noise signal (10) of magnitude $\varepsilon \in \{0, 0.3\}$, for Example 1. The solutions plotted over the value functions are displayed by the dashed red lines with initial conditions denoted by the circles and terminal conditions by the crosses. The setpoints $\mathcal{Z}^*$ are denoted by the red stars.

Specifically, $\pi_2(z) > \pi_1(z)$ for all $z \in [-3, -1.6)$ and $\pi_1(z) < \pi_2(z)$ for all $z \in (1.6, 3]$, as can be seen in Figure 1. Hence, solutions evolve towards z^* quicker under the exploitative selection.[5]

Figure 1 shows that the resulting control policy by applying the supervisory policy Q^* is piecewise continuous. In particular, the resulting control policy changes its decision for a small change in the state z near $z_c := 0$, referred to as a critical state. Recall that $\dot{z} = u$, hence near this critical state, $\dot{z} > 0$ for $z \in (z_c, z_2^*)$ and $\dot{z} < 0$ for $z \in (z_1^*, z_c)$. To highlight the issue near z_c, suppose the system is in the region $z \in (z_c - \varepsilon, z_c)$, where $\varepsilon > 0$. Without measurement noise, the supervisory policy Q^* selects policy π_1 as the system is in the subset of the region $z \in (z_1^*, z_c)$. However, with a small perturbation $m = \varepsilon$, the measured state is in the region $z + m \in (z_c, z_c + \varepsilon)$, placing it in the subset of the region $z \in (z_c, z_2^*)$ and causing the supervisory policy Q^* to select policy π_2. At the next sampling interval, that is, when the supervisory policy Q^* makes its next decision, the system moves to the region $z \in (z_c, z_c + \varepsilon)$ due to the previous selection of policy π_2. This time, with a perturbation $m = -\varepsilon$, the measured state is $z + m \in (z_c - \varepsilon, z_c)$, resulting in the supervisory policy Q^* selecting policy π_1 and pushing the system back into the region $(z_c - \varepsilon, z_c)$. Repetition of this pattern causes the system to chatter around the critical state z_c.[6] *Figure 2b illustrates this chattering behavior. In Figure 2, the solutions to the closed-loop system using the supervisory policy Q^* are shown for various initial conditions in the presence of the measurement noise signal given by*

$$m(t) = \varepsilon m_{\text{sgn}}(t), \tag{10}$$

where $\varepsilon \in \mathbb{R}_{\geq 0}$ is the magnitude of the measurement noise and m_{sgn} is a function that changes its sign at every sampling time interval $\Delta t = 0.05$ and is given by $m_{\text{sgn}}(t) = \text{sgn}\left(\cos\left(\frac{\pi t}{\Delta t}\right)\right)$ for all $t \in \mathbb{R}_{\geq 0}$, where sgn *is the signum function. While Figure 2a shows that all the considered solutions converge to the set $\mathcal{Z}^*$ without measurement noise, Figure 2b illustrates that the measurement noise signal in (10) causes the solutions starting near z_c to chatter around $z = z_c$, thereby preventing those solutions from converging to the set $\mathcal{Z}^*$.*

To address the issue of chattering in the supervisory policy, we propose a value function-based switching approach that ensures the resulting hybrid closed-loop system is robust to measurement noise and preserves the properties of the individual policies.

[5] The supervisory policy Q^* is not necessarily the optimal switching strategy; however, it is probably better or equal to a non-switching strategy.

[6] The decision of the supervisory policy Q^* changes near $z \in \{-1.6, 1.6\}$ as well; however, as both policies have an equal sign for these points, chattering does not occur at these points.

4 Hybrid Supervisor

In this section, we first define a class of systems and establish value function-based conditions that characterize *critical areas*, where multiple policies appear equally "good", and small perturbations can trigger undesired chattering behavior and performance degradation. Using these conditions, we then propose a hybrid supervisor that deploys a timer-based mechanism to predict and enforce a dwell period between policy switches.

4.1 Class of Systems

The focus is on systems where certain regions of the state space, termed *critical areas*, feature multiple locally equally optimal policies. In these critical areas, system decisions become highly sensitive to small perturbations in observations, which can lead to rapid switching between decisions, resulting in undesired chattering behavior and performance degradation. From a value function-based perspective, these critical areas are more formally identified using the following conditions, given a policy bank Π with Lipschitz policies $\pi_q \colon \mathcal{Z} \to \mathcal{U}$ for $q \in \mathcal{Q}$, continuously differentiable approximate value functions $\hat{V}_q \colon \mathcal{Z} \to \mathbb{R}$ of the form (4), and continuous-time dynamics as in (1) with $\mathcal{Z}$ closed, critical areas are identified by the following conditions:

($\circ$) for each $z \in \mathcal{M}^* \subset \mathcal{Z}$, there exist $q, p \in Q^*(z)$, $q \neq p$, such that

$$\hat{V}_q(z) = \hat{V}_p(z), \tag{11}$$

$$\langle \nabla \hat{V}_q(z), f(z, \pi_q(z)) \rangle > 0 \text{ and } \langle \nabla \hat{V}_p(z), f(z, \pi_p(z)) \rangle > 0, \tag{12}$$

$$\langle \nabla \hat{V}_q(z), f(z, \pi_p(z)) \rangle < 0 \text{ and } \langle \nabla \hat{V}_p(z), f(z, \pi_q(z)) \rangle < 0. \tag{13}$$

Therefore, the set $\mathcal{M}^*$ is defined as

$$\begin{aligned} \mathcal{M}^* := \{ z \in \mathcal{Z} : & \exists q \in Q^*(z), p \in Q^*(z) \setminus \{q\} : \hat{V}_p(z) = \hat{V}_q(z), \\ & \langle \nabla \hat{V}_q(z), f(z, \pi_q(z)) \rangle > 0, \langle \nabla \hat{V}_p(z), f(z, \pi_p(z)) \rangle > 0, \\ & \langle \nabla \hat{V}_q(z), f(z, \pi_p(z)) \rangle < 0, \langle \nabla \hat{V}_p(z), f(z, \pi_q(z)) \rangle < 0 \}. \end{aligned} \tag{14}$$

The conditions in ($\circ$) can be interpreted as follows. Condition (11) identifies states z where multiple policies π_q and π_p are equally optimal, allowing a supervisory policy to select either q or p. Condition (12) indicates that the value functions $\hat{V}_q$ and $\hat{V}_p$ increase locally when following their respective policies π_q and π_p. Conversely, condition (13) shows that the value functions decrease when following the opposing policies π_p and π_q, respectively. Together, these conditions are used to define the following partitions of the state space $\mathcal{Z}$ near the critical areas $\mathcal{M}^*$.

Lemma 1. *Under the conditions in* ($\circ$)*, there exists $\delta > 0$ such that the set $\mathcal{M}^*$ satisfies*

$$\bigcup_{q \in \mathcal{Q}'} \mathcal{Z}_q = \mathcal{Z} \cap (\mathcal{M}^* + \delta \mathbb{B}), \tag{15}$$

where $\mathcal{Q}' := \bigcup_{z \in \mathcal{M}^*} Q^*(z) \subset \mathcal{Q}$ and, for each $q \in \mathcal{Q}'$, the partition

$$\mathcal{Z}_q := \bigcap_{p \in \mathcal{Q}' \setminus \{q\}} \{ z \in \mathcal{Z} \cap (\mathcal{M}^* + \delta \mathbb{B}) : \hat{V}_q(z) - \hat{V}_p(z) \geq 0 \} \tag{16}$$

satisfies

(A1) *$\mathcal{Z}_q$ is closed for each $q \in \mathcal{Q}'$;*

(A2) *$\hat{V}_q(z) > \hat{V}_p(z)$ for all $z \in \operatorname{int}(\mathcal{Z}_q)$ and $p \in \mathcal{Q}' \setminus \{q\}$; and*

(A3) *$\operatorname{int}(\mathcal{Z}_q) \cap \operatorname{int}(\mathcal{Z}_p) = \varnothing$ for all $q, p \in \mathcal{Q}'$, $p \neq q$.*

The proof of Lemma 1 can be found in the supplementary material.

By Lemma 1, there exists $\delta > 0$ such that the neighborhood $\mathcal{M}^* + \delta\mathbb{B}$ is partitioned into regions $\mathcal{Z}_q$ with disjoint interiors, where each $\mathcal{Z}_q$ corresponds to a region where $\hat{V}_q$ is strictly larger than $\hat{V}_p$ for all $q, p \in \mathcal{Q}'$, $p \neq q$. Suppose, without loss of generality, that $z \in \mathcal{Z}_q$ for some $q \in \mathcal{Q}'$. Then, due to the properties in Lemma 1, every point $z \in \mathcal{M}^* + \delta\mathbb{B}$ is δ close to some boundary between $\mathcal{Z}_q$ and $\mathcal{Z}_p$. Therefore, there exists a perturbation $m \in \delta\mathbb{B}$, for which the perturbed state $z + m$ belongs to $\mathcal{Z}_p$. Consequently, even though z initially lies in $\mathcal{Z}_q$, the perturbation leads to the selection of policy π_p. Since $z + m$ is in $\mathcal{M}^* + \delta\mathbb{B}$, conditions (12) and (13) ensure that if p is chosen in $\mathcal{Z}_q$, $\hat{V}_p$ increases while $\hat{V}_q$ decreases, effectively making $\mathcal{M}^*$ attractive. That is, the system is "pulled" back toward the critical area. Subsequent perturbations can then induce a switch back to q, leading to chattering between policies near the critical area.

4.2 Timer-based Hybrid Supervisor

The hybrid supervisor employs a timer to prevent chattering near critical areas. This timer-based approach sets a dwell time parameter based on the value functions and a noise-free model of the system dynamics, ensuring a minimum waiting period before another policy switch is allowed.

The hybrid closed-loop system $\mathcal{H} = (C, F, D, G)$ models the continuous evolution (flow) and discrete updates (jumps) of its state, which consists of the system state z of (1), a timer $\tau \in \mathbb{R}_{\geq 0}$, the logic variable $q \in \{1, 2, \ldots, N\} =: \mathcal{Q}$, where $N \in \mathbb{N}_{>0}$ is the number of policies in the policy bank, and an adjustable dwell time parameter $\delta_d \in \mathbb{R}_{>0}$. The adjustable dwell time parameter δ_d dictates the amount of time that needs to elapse before the applied policy can be changed, namely, to change q. The state is defined as $x = (z, \tau, q, \delta_d) \in \mathcal{X} := \mathcal{Z} \times \mathbb{R}_{\geq 0} \times \mathcal{Q} \times \mathbb{R}_{\geq 0}$. The flow map F governs the continuous evolution of each state component, the flow set C specifies the conditions under which the state components can flow, the jump map G governs the discrete updates, and the jump set D defines the conditions under which the state components can jump.

During flows, the state z evolves according to its dynamics (1) under the selected policy π_q from the policy bank. Furthermore, the policy decision stored in q and the adjustable dwell time parameter δ_d do not change during flows. On the other hand, the timer τ evolves linearly with a constant rate of one so as to count ordinary time. The *flow map* F that captures this behavior is given by

$$\begin{bmatrix} \dot{z} \\ \dot{\tau} \\ \dot{q} \\ \dot{\delta}_d \end{bmatrix} = F(x) := \begin{bmatrix} f(z, \pi_q(z)) \\ 1 \\ 0 \\ 0 \end{bmatrix} \quad x \in C. \tag{17}$$

The system flows whenever the timer τ is less than or equal to the adjustable dwell time parameter δ_d, or when the logic variable q corresponds to the highest value function for the current value of the state z, leading to the *flow set* $C := C_0 \cup C_1$, where

$$\begin{aligned} C_0 &:= \{x \in \mathcal{X} : \tau \leq \delta_d\}; \\ C_1 &:= \{x \in \mathcal{X} : q \in Q^*(z)\}, \end{aligned} \tag{18}$$

where Q^* is given by (9). The *jump map* G is given by

$$\begin{bmatrix} z^+ \\ \tau^+ \\ q^+ \\ \delta_d^+ \end{bmatrix} \in G(x) := \begin{bmatrix} z \\ 0 \\ \left\{ \begin{bmatrix} q' \\ \min\left(\mathcal{T}(z, q') \cup \{\bar{\delta}_d\}\right) \end{bmatrix} : q' \in Q^*(z) \right\} \end{bmatrix} \quad x \in D, \tag{19}$$

where

$$\begin{aligned} \mathcal{T}(z, q) := \Big\{ \eta \in [0, \bar{\delta}_d] : & \frac{\max\limits_{\bar{q} \in (\mathcal{Q} \setminus \{q\})} \hat{V}_{\bar{q}}(\chi(\eta)) - \hat{V}_q(\chi(\eta))}{|\hat{V}_q(\chi(\eta))| + \epsilon} \geq \mu, \\ & \text{where } \dot{\chi} = f(\chi, \pi_q(\chi)), \quad \chi(0) = z \Big\}, \end{aligned} \tag{20}$$

where $\epsilon \in \mathbb{R}_{>0}$ is a very small constant (e.g., $\epsilon \ll 1$) used to avoid division by zero, $\mu \in \mathbb{R}_{>0}$ is a constant, and $\bar{\delta}_d \in \mathbb{R}_{>0}$ is the maximum value of the dwell time parameter. The set-valued map $\mathcal{T}\colon \mathcal{Z} \rightrightarrows [0, \bar{\delta}_d]$ gathers all time horizons up to $\bar{\delta}_d$ at which a *significant* relative improvement (as determined by μ) over the *current* optimal policy q' is predicted. To clarify the construction of the ratio in (20), suppose that, for some $q \in \mathcal{Q}$ and for some $\eta \in [0, \bar{\delta}_d]$, we have $\hat{V}_q(\chi(\eta)) > 0$. Then, the ratio in (20) can be written as

$$\hat{V}_{\bar{q}}(\chi(\eta)) \geq \mu(|\hat{V}_q(\chi(\eta))| + \epsilon) + \hat{V}_q(\chi(\eta)) > (1+\mu)\hat{V}_q(\chi(\eta)), \tag{21}$$

where $\bar{q} \in \mathcal{Q} \setminus \{q\}$. This inequality indicates that the policy with index $\bar{q}$ yields a return that is more than $1+\mu$ times the return of policy q at η seconds in the future. Next, suppose that, for some $q \in \mathcal{Q}$ and for some $\eta \in [0, \bar{\delta}_d]$, we have $\hat{V}_q(\chi(\eta)) < 0$. In this case, the ratio in (20) can be written as

$$\hat{V}_{\bar{q}}(\chi(\eta)) - \hat{V}_q(\chi(\eta)) \geq \mu(|\hat{V}_q(\chi(\eta))| + \epsilon) > \mu|\hat{V}_q(\chi(\eta))|, \tag{22}$$

where again $\bar{q} \in \mathcal{Q} \setminus \{q\}$. Here, the inequality shows that the difference in return between the policy with index $\bar{q}$ and the policy with index q is greater than μ times the return of policy q at η seconds in the future. Notice that the absolute value in the term $|\hat{V}_q(\chi(\eta))|$ is essential. To illustrate this, suppose again that, for some $q \in \mathcal{Q}$ and for some $\eta \in [0, \bar{\delta}_d]$, we have $\hat{V}_q(\chi(\eta)) < -\epsilon$. In this case, if we were to omit the absolute value, the ratio in (20) would be written as

$$\hat{V}_{\bar{q}}(\chi(\eta)) \leq \mu\Big(\hat{V}_q(\chi(\eta)) + \epsilon\Big) + \hat{V}_q(\chi(\eta)) = (\mu+1)\hat{V}_q(\chi(\eta)) + \mu\epsilon. \tag{23}$$

Since $\hat{V}_q(\chi(\eta)) < -\epsilon$, the sum $\hat{V}_q(\chi(\eta)) + \epsilon$ is negative, which makes the right-hand side of (23) negative as well. This means that the inequality would hold even if the return of policy $\bar{q}$ is actually *worse* than $1+\mu$ times the return of policy q at η seconds in the future. By including the absolute value, we ensure a meaningful comparison of returns regardless of the sign of $\hat{V}_q(\chi(\eta))$.

The constant $\epsilon > 0$ ensures the ratio is well-defined even when $\hat{V}_q(\chi(\eta))$ is close to zero. In (20), the trajectory $\chi(\eta)$ with $\chi(0) = z$ is a solution of $\dot{\chi} = f(\chi, \pi_q(\chi))$ for $\eta \in [0, \bar{\delta}_d]$. For each alternative policy $\pi_{\bar{q}}$ with $\bar{q} \in \mathcal{Q} \setminus \{q\}$, we compare $\hat{V}_q(\chi(\eta))$ with $\hat{V}_{\bar{q}}(\chi(\eta))$. Whenever the resulting ratio meets or exceeds the threshold μ, the corresponding η is included in $\mathcal{T}(z, q)$. In (19), it can be seen that, at jumps, the state z remains unchanged, and the logic variable q is updated to correspond to the index of one of the value functions with largest value, that is q is reset to a point in $Q^*(z)$, therefore the system inherits the properties of the corresponding individual controller during the subsequent period of flow. The timer τ is reset to 0, and the adjustable dwell time parameter δ_d is reset to the minimum between the smallest time horizon in $\mathcal{T}(z, q)$ or to the maximum dwell time $\bar{\delta}_d$. If the set $\mathcal{T}(z, q)$ is empty, which is possible when no significant improvement is observed over the current optimal policy within the time horizon δ_d, then δ_d is reset to $\bar{\delta}_d$.

The system jumps whenever the state is in the *jump set* D, which is defined as

$$D := \{x \in \mathcal{X} : \tau \geq \delta_d\,, q \in \mathcal{Q} \setminus Q^*(z)\}. \tag{24}$$

In (24), it can be seen that the jump in (19) occurs whenever the timer is greater than or equal to the adjustable dwell time parameter δ_d and the logic variable q does not correspond to a value function with the largest value.

Next, the key properties of the hybrid closed-loop system $\mathcal{H}$ in (17)-(24) are discussed. The first property, namely the hybrid basic conditions, is a set of mild conditions on the data (C, F, D, G) of the hybrid closed-loop system $\mathcal{H}$. These conditions are required to ensure that asymptotically stable compact sets of the hybrid closed-loop system $\mathcal{H}$ are robust against disturbances.

Proposition 1. *The hybrid closed-loop system $\mathcal{H}$ in (17)-(24) satisfies the hybrid basic conditions if, for each $q \in \mathcal{Q}$, the approximate value function $\hat{V}_q\colon \mathcal{Z} \to \mathbb{R}$ in (4) is continuous and the policy $\pi_q\colon \mathcal{Z} \to \mathcal{U}$ and $f\colon \mathcal{Z} \times \mathcal{U} \to \mathcal{Z}$ are Lipschitz continuous.*

The proof of Proposition 1 can be found in the supplementary material.

The following proposition shows that under mild continuity and Lipschitz conditions, the hybrid closed-loop system $\mathcal{H}$ in (17)-(24) has nontrivial solutions for every initial state in the flow or jump set. Without this guarantee, the algorithm could get stuck, preventing further progress.

Proposition 2. *Suppose, for each $q \in \mathcal{Q}$, the approximate value function $\hat{V}_q \colon \mathcal{Z} \to \mathbb{R}$ in (4) is continuous and the policy $\pi_q \colon \mathcal{Z} \to \mathcal{U}$ and $f \colon \mathcal{Z} \times \mathcal{U} \to \mathcal{Z}$ are Lipschitz continuous. Then, for each $x_\circ \in C \cup D$, there exists a nontrivial solution x to the hybrid closed-loop system $\mathcal{H}$ in (17)-(24) with $x(0,0) = x_\circ$. Furthermore, every maximal solution x to $\mathcal{H}$ is complete and not Zeno, and every bounded solution x to $\mathcal{H}$ has jump times that are uniformly lower bounded by a positive constant,[7] that is, for each bounded solution x to $\mathcal{H}$ there exists $\beta > 0$ such that $t_{j+1} - t_j \geq \beta$ for all $j \geq 1$, where t_j denotes the time at jump j.*

The proof of Proposition 2 can be found in the supplementary material.

The following theorem demonstrates that, under mild assumptions, the hybrid closed-loop system $\mathcal{H}$ in (17)-(24) solves problem ($\star$). This implies the hybrid supervisor not only maintains the global asymptotic stability properties of the underlying policies but also prevents chattering between the policies when subjected to small, bounded measurement noise. This robustness to chattering stems from the enforced separation of switching boundaries and the regularity of the flow map (17).

Theorem 1. *Suppose, for each $q \in \mathcal{Q}$, the approximate value function $\hat{V}_q \colon \mathcal{Z} \to \mathbb{R}$ in (4) is continuous and the policy $\pi_q \colon \mathcal{Z} \to \mathcal{U}$ and $f \colon \mathcal{Z} \times \mathcal{U} \to \mathcal{Z}$ are Lipschitz continuous. Furthermore, each policy $\pi_q \in \Pi$ globally asymptotically stabilizes[8] a compact set $\mathcal{Z}_q^*$, where $\mathcal{Z}^* := \bigcup_{q \in \mathcal{Q}} \mathcal{Z}_q^*$, and, for each $q \in \mathcal{Q}$, the corresponding value function $\hat{V}_q$ attains its global maximum at $\mathcal{Z}_q^*$ and strictly decreases as the distance from $\mathcal{Z}_q^*$ increases. Then, the hybrid closed-loop system $\mathcal{H}$ in (17)-(24) solves Problem ($\star$).*

The proof of Theorem 1 can be found in the supplementary material.

Example 2 (Stabilizing two disconnected points on a line, revisited)**.** *The solutions of the hybrid closed-loop system $\mathcal{H}$ in (17)-(24) are shown in Figure 3 for various initial conditions in the presence of the measurement noise signal (10) of magnitude $\varepsilon \in \{0, 0.3\}$. Furthermore, the parameters in the jump set (24) are chosen as $\mu = 0.1$ and $\bar{\delta}_d = 0.5$.[9] Figure 3b shows that the hybrid closed-loop system $\mathcal{H}$ in (17)-(24) is robust against the perturbation that caused the switching logic (9) in Example 1 Figure 2b to chatter. Furthermore, the rapid policy switching that occurs near $z \in \{-1.5, 1.5\}$ in Figure 2b is also prevented by the hybrid switching logic.*

4.3 Design Considerations

The timer-based approach relies on predicting the system state using a dynamic model, which can be computationally expensive. The maximum dwell time $\bar{\delta}_d$ in (19) sets the upper limit for the prediction horizon. If $\bar{\delta}_d$ is set too low, the prediction horizon may be insufficient for the system to exit critical areas, thereby reducing robustness; if it is set too high, the increased computational cost—and, when combined with a high threshold parameter μ in (20), the potential for prolonged adherence to a suboptimal policy—may degrade performance. The parameter μ serves as a safeguard against rapid switching when the value functions of competing policies are nearly equal. Together, $\bar{\delta}_d$ and μ balance the trade-off between computational efficiency, exploitative policy switching, and robustness.

As a practical guideline, the maximum dwell time $\bar{\delta}_d$ should be selected such that the system has sufficient time for its state z to move away from critical areas by an amount distinguishable from, or ideally exceeding, the expected magnitude of measurement noise $\varepsilon \in \mathbb{R}_{\geq 0}$. Concretely, pick $\bar{\delta}_d$

[7] Under the assumptions in Theorem 1, every maximal solution is bounded.

[8] "*Globally asymptotically stabilizes*" means that for each individual policy $\pi_q \in \Pi$, the set $\mathcal{Z}_q^*$ is asymptotically stable and its region of attraction is the entire state space $\mathcal{Z}$.

[9] The design/choice of μ and $\bar{\delta}_d$ is discussed in Section 4.3.

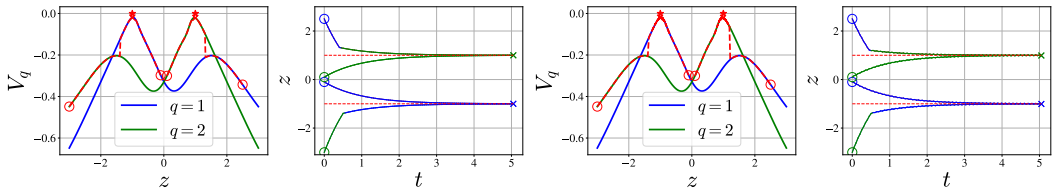

(a) Noise magnitude $\varepsilon = 0$.

(b) Noise magnitude $\varepsilon = 0.3$.

Figure 3: The solutions of the hybrid closed-loop system $\mathcal{H}$ in (17)-(24), where $\mu = 0.1$ and $\bar{\delta}_d = 0.5$, over the approximate value function $\hat{V}_1$, in blue, and $\hat{V}_2$, in green, for the policies π_1 and π_2, respectively, and over time under the measurement noise signal (10) of magnitude $\varepsilon \in \{0, 0.3\}$, for Example 1. The solutions plotted over the value functions are displayed by the dashed red lines with initial conditions denoted by the circles and terminal conditions by the crosses. The setpoints $\mathcal{Z}^*$ are denoted by the red stars.

such that

$$\bar{\delta}_d > \frac{\varepsilon}{\max_{(z,u)\in X} |f(z,u)|}, \tag{25}$$

where $f\colon \mathcal{Z} \times \mathcal{U} \to \mathcal{Z}$ is given by (1) and $X \subset \mathcal{Z} \times \mathcal{U}$ is a compact set. Additionally, the threshold parameter μ should be chosen to exceed the worst-case fractional perturbation in the value function caused by measurement noise. Specifically, pick μ such that

$$\mu > \frac{\varepsilon L_{\hat{V}}}{|\hat{V}_{\text{ref}}|}, \tag{26}$$

where $L_{\hat{V}_q}$ is the Lipschitz constant of the value function $\hat{V}_q$, satisfying $|\hat{V}_q(z_1) - \hat{V}_q(z_2)| \leq L_{\hat{V}_q}|z_1 - z_2|$ for all $z_1, z_2 \in \mathcal{Z}$. Letting $L_{\hat{V}} := \max_{q\in\mathcal{Q}} L_{\hat{V}_q}$, it follows that for measurement noise m on state z with magnitude $|m| = \varepsilon$ for which $z + m \in \mathcal{Z}$, the value function perturbation $|\hat{V}_q(z+m) - \hat{V}_q(z)|$ is bounded by $L_{\hat{V}}\varepsilon$. Thus, the term $\varepsilon L_{\hat{V}}$ in (26) represents an upper bound on this noise-induced perturbation for any $\hat{V}_q$.[10] Furthermore, $\hat{V}_{\text{ref}} \in \mathbb{R}_{>0}$ serves as a positive scaling factor representing a characteristic magnitude of the value function $|\hat{V}_q(z)|$ for $z \in \mathcal{Z}$. This normalization is crucial because the magnitude of the measurement noise, such as $\varepsilon = 1$, might be highly significant if the typical range of the value function is 0 to 1, but almost inconsequential if its range is 0 to 1000. Thus, by normalizing $\varepsilon L_{\hat{V}}$ with $\hat{V}_{\text{ref}}$ in (26), μ can be interpreted as a threshold for the fractional change in the value function. Common choices for $\hat{V}_{\text{ref}}$ include the maximum or average value of $|\hat{V}_q(z)|$ for $z \in \mathcal{Z}$.

5 Application

We consider a system evolving on a plane with the state $z = (z_x, z_y) \in \mathcal{Z} \subset \mathbb{R}^2$, with $z_x \in \mathbb{R}$ and $z_y \in \mathbb{R}$ being the coordinates along the $x-$ and $y-$axes, respectively, and dynamics $\dot{z} = u$, where $u \in [-1, 1]^2$ is the control input. The problem to solve consists of robustly globally asymptotically stabilizing the set $\mathcal{Z}^* := \{z_1^*, z_2^*, z_3^*, z_4^*\} := \{(-1, 0.2), (-0.1, 1), (0.9, -0.1), (-0.4, -0.9)\} \subset \mathcal{Z}$, which consists of four disconnected setpoints, by designing a supervisory policy to select between the four available policies, π_1, π_2, π_3 and π_4, based on the observation vector $o(z + m) = z + m$, where $m \in \mathbb{R}^2$ represents the measurement noise. The policies are given by (7) for each $z \in \mathcal{Z}$ and each value of the logic variable $q \in \{1, 2, 3, 4\} := \mathcal{Q}$. It can be shown that each policy globally asymptotically stabilizes one of the setpoints, namely, π_1 globally asymptotically stabilizes z_1^*, π_2 globally asymptotically stabilizes z_2^*, π_3 globally asymptotically stabilizes z_3^*, and π_4 globally asymptotically stabilizes z_4^*. The

[10] Under the assumption that $\mathcal{Z}$ is a compact set.

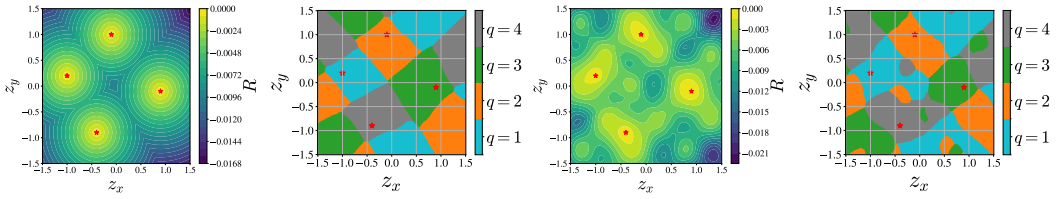

(a) Without periodic variations.

(b) With periodic variations.

Figure 4: Visualization of the reward function (27) (located left in each sub-figure) and Q^* (located right in each sub-figure) without and with the periodic variations. The setpoints $\mathcal{Z}^*$ are denoted by the red stars.

value iteration algorithm is applied to find the approximate value functions $\hat{V}_q$ for $q \in \mathcal{Q}$ subject to the reward function

$$R(z) = -c_1 |z|_{\mathcal{Z}^*} \left(1 + \frac{1}{2}\sin(c_2 z_x)\cos(c_3 z_y)\right), \tag{27}$$

which has a global maximum for $z \in \mathcal{Z}^*$, where $c_1, c_2, c_3 \in \mathbb{R}_{>0}$ are constants, discount rate $\rho = -\frac{1}{\Delta t}\ln 0.9$, sampling time of $\Delta t = 0.025$ seconds, and a horizon of 100 time steps. The term $1 + \frac{1}{2}\sin(c_2 z_x)\cos(c_3 z_y)$ introduces periodic variations in the reward function, creating local minima and maxima across the state space. As a result, following the shortest Euclidean path to a setpoint is not necessarily optimal—certain indirect trajectories may yield a higher long-term return. This makes determining the optimal regions for each policy—the regions where a given policy has the highest corresponding value function, namely $\mathcal{Q}^*$ (9)—nontrivial. Consequently, this leads to more complex switching boundaries and decision regions, as shown in Figure 4.

Figure 5 compares the closed-loop system solutions under three different supervisors. The first row shows the supervisory policy Q^*, given by (9); the second row illustrates a fixed-timer approach with a dwell time of $\bar{\delta}_d$ equal to the maximum value of the dwell time parameter used by the timer-based hybrid supervisor; and the third row depicts the timer-based hybrid supervisor. The timer-based hybrid supervisor, introduced in Section 4.2, is given by (17)-(24) with parameters $\bar{\delta}_d = 0.5$ and $\mu = 0.15$. The trajectories are plotted over the optimal policy regions $\mathcal{Q}^*$ and over time under the influence of a measurement noise signal, given by

$$m(t) = \begin{bmatrix} \varepsilon & -\varepsilon \end{bmatrix}^\top m_{\text{sgn}}(t), \tag{28}$$

where the noise magnitude is $\varepsilon \in \{0, 0.1\}$.[11] The first row of Figure 5 shows that the supervisory policy Q^* is highly sensitive to measurement noise, leading to chattering and, in some cases, failure to reach the target set $\mathcal{Z}^*$. Notably, chattering occurs for at least one initial condition even in the absence of noise. The second row indicates that while the fixed-timer supervisor proves robust for most initial conditions, it can become trapped between regions near $z = (-0.25, 0.25)$ and $z = (-0.25, -0.25)$, underscoring that a fixed dwell time does not necessarily guarantee global asymptotic stability of the closed-loop system. In contrast, the third row demonstrates that the hybrid supervisor successfully mitigates chattering and consistently guides the system to $\mathcal{Z}^*$ for all considered initial conditions, even under the same measurement noise that caused instability in Q^*.

Remark. *The problem setup described mirrors many real-world multi-strategy decision-making scenarios, which are often complicated by limited information, long-term trade-offs, and potential adversarial actions designed to induce erroneous or inefficient switching, leading to suboptimal performance. For instance, in strategic interactions like video games, an opponent might exploit uncertainties to bait an agent into frequent, detrimental changes in tactics, for example, between aggressive or defensive postures. Such complexities underscore the critical need for robust strategy selection mechanisms in dynamic and potentially adversarial environments.*

[11] This deterministic noise pattern can be thought of as an adversarial agent designed to induce chattering behavior.

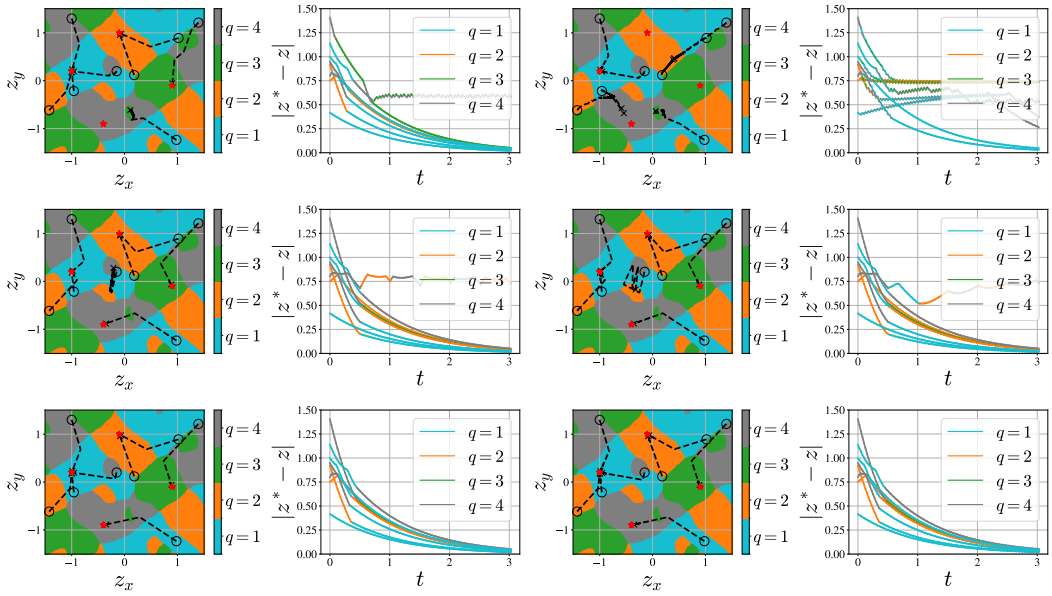

Figure 5: The solutions of the (hybrid) closed-loop system using the supervisory policy Q^* (first row), the fixed-timer supervisor (second row), and the timer-based hybrid supervisor from Section 4.2 (third row), plotted over Q^*, and over time under the measurement noise signal (28) of magnitude $\varepsilon \in \{0, 0.1\}$. The solutions plotted over the optimal regions for each policy are displayed by the black dashed lines with initial conditions denoted by the circles and terminal conditions by the crosses. The solutions plotted over time illustrate when the switches between policies occur. The setpoints $\mathcal{Z}^*$ are denoted by the red stars.

6 Conclusion

This paper presents a novel timer-based hybrid supervisor that leverages value functions for robust switching among multiple policies. The supervisor predicts and enforces a minimum dwell time between policy switches, thereby preventing chattering even under bounded measurement noise and assuring asymptotic stability. Sufficient conditions are presented for non-Zeno behavior and robust asymptotic stability of the hybrid closed-loop system. Numerical simulations on representative decision-making problems demonstrate that the supervisor effectively mitigates rapid switching and drives the system toward the desired target set even under noisy conditions, where a conventional switching strategy fails.

Acknowledgments

The authors would like to thank Zachary I. Bell for insightful discussions during the initial stages of this work.

Research by J. de Priester and R. G. Sanfelice has been partially supported by the National Science Foundation under Grant nos. CNS-2039054 and CNS-2111688, by the Air Force Office of Scientific Research under Grant nos. FA9550-23-1-0145, FA9550-23-1-0313, and FA9550-23-1-0678, by the Air Force Research Laboratory under Grant nos. FA8651-22-1-0017 and FA8651-23-1-0004, by the Army Research Office under Grant no. W911NF-20-1-0253, and by the Department of Defense under Grant no. W911NF-23-1-0158.

References

Tansu Alpcan and Tamer Baar. *Network Security: A Decision and Game-Theoretic Approach*. Cambridge University Press, USA, 1st edition, 2010. ISBN 0521119324.

Söhnke M Bartram, Jürgen Branke, Giuliano De Rossi, and Mehrshad Motahari. Machine learning for active portfolio management. *Journal of Financial Data Science*, 3(3):9–30, 2021.

Yassine Chemingui, Aryan Deshwal, Honghao Wei, Alan Fern, and Jana Doppa. Constraint-adaptive policy switching for offline safe reinforcement learning. In *Proceedings of the AAAI Conference on Artificial Intelligence*, volume 39, pp. 15722–15730, 2025.

Jan de Priester, Ricardo G. Sanfelice, and Nathan van de Wouw. Hysteresis-based rl: Robustifying reinforcement learning-based control policies via hybrid control. In *2022 American Control Conference (ACC)*, pp. 2663–2668, 2022. DOI: 10.23919/ACC53348.2022.9867627.

Jan de Priester, Zachary Bell, Prashant Ganesh, and Ricardo Sanfelice. MultiHyRL: Robust hybrid RL for obstacle avoidance against adversarial attacks on the observation space. *Reinforcement Learning Journal*, 4:2017–2040, 2024.

Rafal Goebel, Ricardo G. Sanfelice, and Andrew R. Teel. *Hybrid Dynamical Systems: Modeling, Stability, and Robustness*. Princeton University Press, 2012. ISBN 9780691153896. URL http://www.jstor.org/stable/j.ctt7s02z.

Max L. Greene, Moad Abudia, Rushikesh Kamalapurkar, and Warren E. Dixon. Model-based reinforcement learning for optimal feedback control of switched systems. In *2020 59th IEEE Conference on Decision and Control (CDC)*, pp. 162–167, 2020. DOI: 10.1109/CDC42340.2020.9304400.

Jemin Hwangbo, Joonho Lee, Alexey Dosovitskiy, Dario Bellicoso, Vassilios Tsounis, Vladlen Koltun, and Marco Hutter. Learning agile and dynamic motor skills for legged robots. *Science Robotics*, 4(26):eaau5872, 2019. DOI: 10.1126/scirobotics.aau5872. URL https://www.science.org/doi/abs/10.1126/scirobotics.aau5872.

Hassan K Khalil. *Nonlinear systems; 3rd ed.* Prentice-Hall, Upper Saddle River, NJ, 2002. URL https://cds.cern.ch/record/1173048. The book can be consulted by contacting: PH-AID: Wallet, Lionel.

Wanjiku A. Makumi, Max L. Greene, Zachary I. Bell, Scott Nivison, Rushikesh Kamalapurkar, and Warren E. Dixon. Hierarchical reinforcement learning-based supervisory control of unknown nonlinear systems. *IFAC-PapersOnLine*, 56(2):6871–6876, 2023. ISSN 2405-8963. DOI: https://doi.org/10.1016/j.ifacol.2023.10.485. URL https://www.sciencedirect.com/science/article/pii/S2405896323008522. 22nd IFAC World Congress.

C. G. Mayhew, R. G. Sanfelice, and A. R. Teel. Quaternion-based hybrid controller for robust global attitude tracking. *IEEE Transactions on Automatic Control*, 56(11):2555–2566, November 2011. DOI: http://ieeexplore.ieee.org/xpl/freeabs_all.jsp?arnumber=5701762. URL https://hybrid.soe.ucsc.edu/files/preprints/50.pdf.

Christophe Prieur, Rafal Goebel, and Andrew R. Teel. Hybrid feedback control and robust stabilization of nonlinear systems. *IEEE Transactions on Automatic Control*, 52(11):2103–2117, 2007. DOI: 10.1109/TAC.2007.908320.

Martin L. Puterman. *Markov Decision Processes: Discrete Stochastic Dynamic Programming*. John Wiley & Sons, Inc., USA, 1st edition, 1994. ISBN 0471619779.

R.T. Rockafellar, M. Wets, and R.J.B. Wets. *Variational Analysis*. Grundlehren der mathematischen Wissenschaften. Springer Berlin Heidelberg, 2009. ISBN 9783540627722. URL https://books.google.com/books?id=w-NdOE5fD8AC.

R. G. Sanfelice. *Hybrid Feedback Control*. Princeton University Press, New Jersey, 2021.

John Schulman, Filip Wolski, Prafulla Dhariwal, Alec Radford, and Oleg Klimov. Proximal policy optimization algorithms. *CoRR*, abs/1707.06347, 2017. URL http://arxiv.org/abs/1707.06347.

Georgios N. Yannakakis and Julian Togelius. *Artificial Intelligence and Games*. Springer Publishing Company, Incorporated, 1st edition, 2018. ISBN 3319635182.

Supplementary Materials

The following content was not necessarily subject to peer review.

Proof of Lemma 1. The proof consists of two main parts. First, we establish the equality in (15), namely, $\bigcup_{q\in\mathcal{Q}'} \mathcal{Z}_q = \mathcal{Z} \cap (\mathcal{M}^* + \delta\mathbb{B})$. Second, we demonstrate that the partitions $\mathcal{Z}_q$ satisfy the conditions (A1)-(A3) for each $q \in \mathcal{Q}'$.

To prove the equality in (15), we need to show that the following two set inclusions hold.

(I1) $\bigcup_{q\in\mathcal{Q}'} \mathcal{Z}_q \subseteq \mathcal{Z} \cap (\mathcal{M}^* + \delta\mathbb{B})$; and

(I2) $\mathcal{Z} \cap (\mathcal{M}^* + \delta\mathbb{B}) \subseteq \bigcup_{q\in\mathcal{Q}'} \mathcal{Z}_q$.

To show that (I1) holds, pick any $z_\circ \in \bigcup_{q\in\mathcal{Q}'} \mathcal{Z}_q$. By the definition of the union of sets, it holds that there exists at least one index $q_\circ \in \mathcal{Q}'$ such that $z_\circ \in \mathcal{Z}_{q_\circ}$. By the definition of $\mathcal{Z}_q$ in (16), any element $z_\circ \in \mathcal{Z}_{q_\circ}$ must satisfy the condition $z_\circ \in \mathcal{Z} \cap (\mathcal{M}^* + \delta\mathbb{B})$. Thus $z_\circ \in \mathcal{Z} \cap (\mathcal{M}^* + \delta\mathbb{B})$. Since $z_\circ$ was picked as an arbitrary element from $\bigcup_{q\in\mathcal{Q}'} \mathcal{Z}_q$, the inclusion in (I1) holds.

To show that (I2) holds, pick any $z_\circ \in \mathcal{Z} \cap (\mathcal{M}^* + \delta\mathbb{B})$. The set of indices $\mathcal{Q}' = \cup_{z\in\mathcal{M}^*} Q^*(z)$ is a subset of the finite set $\mathcal{Q}$ and is non-empty as the conditions in ($\circ$) imply the existence of elements in $\mathcal{M}^*$, and for any $z \in \mathcal{M}^*$, $Q^*(z)$ is non-empty. Consider the finite set $\{\hat{V}_{q'}(z_\circ) : q' \in \mathcal{Q}'\}$ that must contain a maximum as $\mathcal{Q}'$ is finite. Let $q^* \in \mathcal{Q}'$ be an index for which this maximum is achieved, such that

$$\hat{V}_{q^*}(z_\circ) = \max_{q'\in\mathcal{Q}'} \hat{V}_{q'}(z_\circ). \tag{29}$$

The choice of q^* in (29) implies that $\hat{V}_{q^*}(z_\circ) \geq \hat{V}_p(z_\circ)$ for each $p \in \mathcal{Q}' \setminus \{q^*\}$. Consequently, for each $p \in \mathcal{Q}' \setminus \{q^*\}$, it holds that $\hat{V}_{q^*}(z_\circ) - \hat{V}_p(z_\circ) \geq 0$. As we picked $z_\circ \in \mathcal{Z} \cap (\mathcal{M}^* + \delta\mathbb{B})$ and $z_\circ$ satisfies $\hat{V}_{q^*}(z_\circ) - \hat{V}_p(z_\circ) \geq 0$ for each $p \in \mathcal{Q}' \setminus \{q^*\}$, $z_\circ$ fulfills all the conditions for membership of the set $\mathcal{Z}_{q^*}$ as defined in (16). Therefore, $z_\circ \in \mathcal{Z}_{q^*}$, which implies that $z_\circ \in \bigcup_{q\in\mathcal{Q}'} \mathcal{Z}_q$. As $z_\circ$ was picked as an arbitrary element from $\mathcal{Z} \cap (\mathcal{M}^* + \delta\mathbb{B})$, the inclusion in (I2) holds.

As both the inclusions (I1) and (I2) hold, the equality in (15) is proven.

For each fixed $q \in \mathcal{Q}'$, consider any $p \in \mathcal{Q}' \setminus \{q\}$. Since both $\hat{V}_q$ and $\hat{V}_p$ are continuous, the function

$$g_p(z) := \hat{V}_q(z) - \hat{V}_p(z) \quad \forall z \in \mathcal{Z} \tag{30}$$

is continuous. Moreover, the set $\mathcal{Z}$ is closed, and since $\mathbb{B}$ is closed, the set $\mathcal{M}^* + \delta\mathbb{B}$ is closed as well. The intersection of these two closed sets, which we denote by $\mathcal{D} := \mathcal{Z} \cap (\mathcal{M}^* + \delta\mathbb{B})$, is therefore closed. Consequently, the set

$$S_p := \{z \in \mathcal{D} : g_p(z) \geq 0\}, \tag{31}$$

is also closed. To show that S_p is closed, note that the condition $g_p(z) \geq 0$ is equivalent to $g_p(z) \in \mathbb{R}_{\geq 0}$. Since $g_p : \mathcal{Z} \to \mathbb{R}$ is continuous and $\mathbb{R}_{\geq 0}$ is a closed subset of $\mathbb{R}$, its preimage $S'_p := \{z \in \mathcal{Z} : g_p(z) \in \mathbb{R}_{\geq 0}\}$ is closed in $\mathcal{Z}$. The set S_p is then the intersection $\mathcal{D} \cap S'_p$. As both $\mathcal{D}$ and S'_p are closed sets, their intersection S_p is also closed. Since $\mathcal{Z}_q$ in (16) is an intersection of finitely many closed sets, it follows that $\mathcal{Z}_q$ is closed for each $q \in \mathcal{Q}'$. Thus, condition (A1) is satisfied.

Furthermore, the set $\mathcal{Z}_q$ can be written as

$$\mathcal{Z}_q = \bigcap_{p\in\mathcal{Q}'\setminus\{q\}} \{z \in \mathcal{Z} \cap (\mathcal{M}^* + \delta\mathbb{B}) : \hat{V}_q(z) - \hat{V}_p(z) \geq 0\} = \bigcap_{p\in\mathcal{Q}'\setminus\{q\}} S_p. \tag{32}$$

The interior of $\mathcal{Z}_q$ is therefore

$$\begin{aligned}
\text{int}\,(\mathcal{Z}_q) &= \text{int}\left(\bigcap_{p\in\mathcal{Q}'\setminus\{q\}} S_p\right); && \text{(33a)}\\
&= \bigcap_{p\in\mathcal{Q}'\setminus\{q\}} \text{int}\,(S_p); && \text{(33b)}\\
&= \bigcap_{p\in\mathcal{Q}'\setminus\{q\}} \text{int}\,(\{z\in\mathcal{D} : g_p(z)\geq 0\}); && \text{(33c)}\\
&= \bigcap_{p\in\mathcal{Q}'\setminus\{q\}} \{z\in\text{int}\,(\mathcal{D}) : g_p(z) > 0\}; && \text{(33d)}\\
&= \bigcap_{p\in\mathcal{Q}'\setminus\{q\}} \{z\in\text{int}\,(\mathcal{D}) : \hat{V}_q(z) - \hat{V}_p(z) > 0\}. && \text{(33e)}
\end{aligned}$$

Hence, for each $z\in\text{int}\,(\mathcal{Z}_q)$, it holds that $\hat{V}_q(z) > \hat{V}_p(z)$, proving condition (A2).

Proceeding by contradiction, suppose that there exists a point

$$z\in\text{int}\,(\mathcal{Z}_q)\cap\text{int}\,(\mathcal{Z}_p) \tag{34}$$

for distinct $q, p\in\mathcal{Q}'$. Then by (A2), since $z\in\text{int}\,(\mathcal{Z}_q)$ we have

$$\hat{V}_q(z) > \hat{V}_p(z), \tag{35}$$

and since $z\in\text{int}\,(\mathcal{Z}_p)$ we have

$$\hat{V}_p(z) > \hat{V}_q(z). \tag{36}$$

This contradiction shows that such a z cannot exist, so

$$\text{int}\,(\mathcal{Z}_q)\cap\text{int}\,(\mathcal{Z}_p) = \varnothing. \tag{37}$$

Thus, condition (A3) is satisfied. □

Proof of Proposition 1. According to Sanfelice (2021, Theorem 2.20), $\mathcal{H}$ satisfies the hybrid basic conditions if

(B1) C and D are closed subsets of $\mathcal{X}$;

(B2) F is outer semicontinuous and locally bounded relative to C, $C\subset$ dom F, and $F(x)$ is convex for each $x\in C$;

(B3) G is outer semicontinuous and locally bounded relative to D, and $D\subset$ dom G.

By definition, the flow set C in (18) and the jump set D in (24) are closed subsets of $\mathcal{X}$, satisfying condition (B1).

The flow map F in (17) is a single-valued map. By assumption, the policies π_q and state dynamics f are Lipschitz continuous for each $q\in\mathcal{Q}$. Furthermore, the policies π_q and state dynamics f are defined for each $z\in\mathcal{Z}$ by assumption. These assumptions ensure that F is continuous on C. Consequently:

- The domain of F satisfies $C\subset$ dom $F=\mathcal{X}$;
- The continuity of F implies that F is outer semicontinuous;
- The continuity of F also guarantees that F is locally bounded relative to C;
- Since F is a single-value map, $F(x)$ is trivially convex for each $x\in C$.

Thus, condition (B2) is satisfied.

The outer semicontinuity of the jump map G follows from the fact that each state component is outer semicontinuous. Specifically, the z and τ components are trivially continuous and hence outer semicontinuous. For the q component, given $z \in \mathcal{Z}$, $Q^*(z)$ in (9) can be written as

$$Q^*(z) = \{q \in \mathcal{Q} : \nu(z, q) = 0\}, \tag{38}$$

where $\nu(z, q) := \hat{V}_q(z) - \max_{\bar{q} \in \mathcal{Q}} \hat{V}_{\bar{q}}(z)$. For each $q \in \mathcal{Q}$, the function ν is continuous as $\hat{V}_q$ is assumed to be continuous, $\mathcal{Q}$ is a finite set, and the maximum over a finite number of continuous functions is continuous. To show that $Q^* \colon \mathcal{Z} \rightrightarrows \mathcal{Q}$ is outer semicontinuous, pick any $z \in \mathcal{Z}$ and a sequence $z_i \to z$. We need to show that for the sequence $y_i \to y$, where $y_i \in Q^*(x_i)$, it holds that $y \in Q^*(z)$. For each point z_i, it holds that $y_i \in Q^*(z_i)$ and thus $\nu(z_i, y_i) = 0$. As ν is a continuous function, it holds that $\lim_{i\to\infty} \nu(z_i, y_i) = 0$ and $\nu(\lim_{i\to\infty}(z_i, y_i)) = 0$. Hence, $\nu(z, y) = 0$ and thus $y \in Q^*(z)$.

For the δ_d component, given $z \in \mathcal{Z}$ and $q \in \mathcal{Q}$, $\mathcal{T}(z, q)$ in (20) can be written as

$$\mathcal{T}(z, q) = \Big\{\eta \in [0, \bar{\delta}_d] : \varrho(\chi(0), q, \eta) \geq 0, \quad \text{where } \chi(0) = z\Big\}, \tag{39}$$

where $\varrho(\chi(0), q, \eta) = \max\limits_{\bar{q} \in (\mathcal{Q} \setminus \{q\}),\, \dot{\chi} = f(\chi, \pi_q(\chi))} \hat{V}_{\bar{q}}(\chi(\eta)) - \hat{V}_q(\chi(\eta)) - \mu(|\hat{V}_q(\chi(\eta))| + \epsilon)$. The system dynamics f are Lipschitz continuous in χ and uniformly continuous in η, namely, ordinary time, therefore by Khalil (2002, Theorem 3.5), the function ϱ has a continuous dependency on the initial state $\chi(0) = z$. Now, fix an arbitrary $z \in \mathcal{Z}$ and define

$$g(\eta) = \varrho(z, q, \eta) \quad \text{for } \eta \in [0, \bar{\delta}_d]. \tag{40}$$

By definition, the inverse image of the closed set $[0, \infty)$ under g is

$$g^{-1}([0, \infty)) = \{\eta \in [0, \bar{\delta}_d] \mid g(\eta) \geq 0\}, \tag{41}$$

which is exactly how $\mathcal{T}(z, q)$ is defined:

$$\mathcal{T}(z, q) = \{\eta \in [0, \bar{\delta}_d] : \varrho(z, q, \eta) \geq 0\} = g^{-1}([0, \infty)). \tag{42}$$

Since g is continuous (as ϱ is continuous in both z and η) and $[0, \infty)$ is closed, it follows from standard topological results that $g^{-1}([0, \infty))$ is closed. Hence, $\mathcal{T}(z, q)$ is a closed subset of $[0, \bar{\delta}_d]$. Next, we define the graph of the set-valued map $\mathcal{T}$ as

$$\mathrm{gph}(\mathcal{T}) = \{(z, q, \eta) \in \mathcal{Z} \times \mathcal{Q} \times [0, \bar{\delta}_d] : \eta \in \mathcal{T}(z, q)\}. \tag{43}$$

Substituting the definition of $\mathcal{T}(z, q)$, we have

$$\mathrm{gph}(\mathcal{T}) = \{(z, q, \eta) \in \mathcal{Z} \times \mathcal{Q} \times [0, \bar{\delta}_d] : \varrho(z, q, \eta) \geq 0\}. \tag{44}$$

Since $\varrho(z, q, \eta)$ is continuous in both z and η, and $[0, \infty)$ is a closed subset of $\mathbb{R}$, the set

$$\{(z, q, \eta) \in \mathcal{Z} \times \mathcal{Q} \times [0, \bar{\delta}_d] : \varrho(z, q, \eta) \geq 0\} \tag{45}$$

is the inverse image of the closed set $[0, \infty)$ under the continuous mapping $(z, q, \eta) \mapsto \varrho(z, q, \eta)$, and is therefore closed. By Rockafellar et al. (2009, Theorem 5.7), a set-valued map whose graph is closed is outer semicontinuous. Hence, the set-valued map $\mathcal{T} \colon \mathcal{Z} \times \mathcal{Q} \rightrightarrows [0, \bar{\delta}_d]$ is outer semicontinuous. To show that

$$\delta_d^+ = \varsigma(z) = \min(\mathcal{T}(z, q') \cup \{\bar{\delta}_d\}) \tag{46}$$

is outer semicontinuous, pick any $z \in \mathcal{Z}$, any $q' \in Q^*(z)$, and a sequence $z_i \to z$. Suppose that for each z_i we choose

$$y_i = \varsigma(z_i) \in \mathcal{T}(z_i, q' \cup \{\bar{\delta}_d\}, \tag{47}$$

and that $y_i \to y$. We need to show that $y = \varsigma(z)$. Since $\mathcal{T}$ is outer semicontinuous, and $y_i \in \mathcal{T}(z_i) \cup \{\bar{\delta}_d\}$ for all i, it follows that $y \in \mathcal{T}(z, q') \cup \{\bar{\delta}_d\}$. Moreover, by definition, for each z_i the number y_i is the minimum element of the set $\mathcal{T}(z_i, q') \cup \{\bar{\delta}_d\}$, namely,

$$y_i \leq \eta \quad \text{for all } \eta \in \mathcal{T}(z_i, q' \cup \{\bar{\delta}_d\}. \tag{48}$$

Taking the limit as $i \to \infty$, and using the fact that inequalities are preserved in the limit, it follows that

$$y \leq \eta \quad \text{for all } \eta \in \mathcal{T}(z, q') \cup \{\bar{\delta}_d\}. \tag{49}$$

Thus, y is a lower bound of $\mathcal{T}(z, q') \cup \{\bar{\delta}_d\}$. Since $\varsigma(z)$ is defined as the minimum of $\mathcal{T}(z, q') \cup \{\bar{\delta}_d\}$, it holds that $y = \varsigma(z)$. Hence, the δ_d component is outer semicontinuous.

As discussed above, the state components z, τ, and δ_d are continuous on $\mathcal{X}$, hence they are bounded relative to D. The component q is also bounded relative to D as q takes values from a finite set $\mathcal{Q}$.

Lastly, for the q component, by assumption, each $\hat{V}_q$ is continuous and well-defined for all $z \in \mathcal{Z}$, and since $\mathcal{Q}$ is finite and nonempty, the set $Q^*(z)$ is nonempty, and thus the q component is well-defined for all $x \in \mathcal{X}$. For the δ_d component, by definition, $\bar{\delta}_d > 0$. If $\mathcal{T}(z, q')$ is empty, the minimum is $\bar{\delta}_d$, which is trivially defined. If $\mathcal{T}(z, q')$ is nonempty, then $\min(\mathcal{T}(z, q'))$ exists because $\mathcal{T}(z, q')$ is a closed subset of $[0, \bar{\delta}_d]$ as discussed above. Hence, the δ_d is well-defined for all $x \in \mathcal{X}$. Since z remains z, τ resets to 0, each component of $G(x)$ is well-defined for all $x \in \mathcal{X}$, and $D \subset \mathcal{X}$, it holds that $D \subset \mathcal{X} \subset \text{dom } G$.

Thus, the condition (B3) is satisfied. □

Proof of Proposition 2. According to Sanfelice (2021, Proposition 2.34), there exists a nontrivial solution x to the hybrid closed-loop system $\mathcal{H}$ in (17)-(24) for each $x_\circ \in C \cup D$ with $x(0, 0) = x_\circ$ if

(B1) The hybrid closed-loop system $\mathcal{H}$ satisfies the hybrid basic conditions; and

(B2) For each $x_\circ \in C \setminus D$ there exists a neighborhood U of $x_\circ$ such that for every $x \in U \cap (C \setminus D)$,

$$F(x) \cap T_C(x) \neq \varnothing. \tag{50}$$

As F is single-valued, (50) simplifies to

$$F(x) \in T_C(x). \tag{51}$$

Additionally, every maximal solution x to $\mathcal{H}$ is not Zeno, and every bounded solution x to $\mathcal{H}$ has jump times that are uniformly lower bounded by a positive constant if the conditions (B1) and (B2) hold and if

(B3) $G(D) \cap D = \varnothing$.

Lastly, every maximal solution x to $\mathcal{H}$ is complete if the conditions (B1) and (B2) hold, F is globally Lipschitz on C, and

(B4) $G(D) \subset C \cup D$.

By Proposition 1, the hybrid closed-loop system $\mathcal{H}$ in (17)-(24) satisfies the hybrid basic conditions under the assumptions, and therefore condition (B1) is satisfied.

The strict flow set $C \setminus D$ is given by

$$C \setminus D = \{x \in \mathcal{X} : \tau < \delta_d\} \cup \{x \in \mathcal{X} : \tau \geq \delta_d, q \in Q^*(z)\}. \tag{52}$$

Since the set $\{x \in \mathcal{X} : \tau < \delta_d\}$ is open, every point x with $\tau < \delta_d$ is an interior point. Consequently, as such x, there are no constraints on the possible flow directions. For the set $\{x \in \mathcal{X} : \tau \geq \delta_d, q \in Q^*(z)\}$, the value of τ cannot decrease if $\tau = \delta_d$ and the value of q cannot change as $Q^*(z)$ is a finite

subset of $\mathbb{N}$. Hence, the q component of the tangent cone for the set $\{x \in \mathcal{X} : \tau \geq \delta_d, q \in Q^*(z)\}$ is equal to zero and the τ component is equal to $\mathbb{R}_{\geq 0}$ if $\tau = \delta_d$. The resulting tangent cone for $C \setminus D$ is given by

$$T_{C\setminus D}(x) = \begin{cases} \mathbb{R}^{n+3} & \text{if } \tau < \delta_d \\ \mathbb{R}^n \times \{0\} \times \mathbb{R}_{\geq 0} \times \mathbb{R} & \text{if } \tau = \delta_d \\ \mathbb{R}^n \times \{0\} \times \mathbb{R}^2 & \text{if } \tau > \delta_d \end{cases}. \tag{53}$$

For the flow map F in (17) it holds that $F(x) \in T_{C\setminus D}(x)$ for $x \in C \setminus D$. Hence, condition $(B2)$ is satisfied.

By the definition of the jump map G in (19), $q^+ \in Q^*(z)$ and $z^+ = z$ for all $x \in D$. As the jump set D in (24) requires $q \in \mathcal{Q} \setminus Q^*(z)$, it holds that $G(D) \cap D = \varnothing$ and condition (B3) is satisfied. Furthermore, by the definition of the flow set C in (18), $G(D) \subset C$ as $q^+ \in Q^*(z)$, $z^+ = z$, and $\tau^+ = 0$. Hence, $G(D) \subset C \cup D$ and condition (B4) is satisfied.

□

Proof of Theorem 1. To solve Problem $(\star)$, the hybrid closed-loop system $\mathcal{H}$ in (17)-(24) needs to:

(P1) Preserve the properties of the individual policies, namely, inducing asymptotic stability of the compact set $\mathcal{Z}^*$; and

(P2) Prevent chattering under measurement noise by guaranteeing a nonzero robustness margin $\varepsilon > 0$.

To prove condition (P1), we will construct a hybrid Lyapunov function and show a strict decrease during flows and jumps unless the state of the system z is in the compact set $\mathcal{A}$, for which the hybrid Lyapunov function equates to zero. In particular, according to Sanfelice (2021, Definition 3.17), the sets $\mathcal{U}, \mathcal{A} \subset \mathcal{X}$ and the function $\mathcal{L}\colon \mathcal{X} \to \mathbb{R}$ define a Lyapunov function candidate on $\mathcal{U}$ with respect to $\mathcal{A}$ for the hybrid closed-loop system $\mathcal{H} = (C, F, D, G)$ if the following conditions hold:

(L1) $(\overline{C} \cup D \cup G(D)) \cap \mathcal{U} \subset \text{dom } \mathcal{L}$;

(L2) $\mathcal{U}$ contains an open neighborhood of $\mathcal{A} \cap (C \cup D \cup G(D))$;

(L3) $\mathcal{L}$ is continuous on $\mathcal{U}$ and locally Lipschitz on an open set containing $\overline{C} \cap \mathcal{U}$; and

(L4) $\mathcal{L}$ is positive definite on $C \cup D \cup G(D)$ with respect to $\mathcal{A}$.

Consider the Lyapunov candidate function defined by

$$\mathcal{L}(x) = -\hat{V}_q(z) + \hat{V}_q(z_q^*), \tag{54}$$

where $x = (z, q, \tau, \delta_d) \in \mathcal{X}$ and $z_q^* \in \mathcal{Z}_q^*$ is the (possibly nonunique) state at which $\hat{V}_q$ attains its global maximum. To obtain a global result, we choose $\mathcal{U} = \mathcal{X}$. Furthermore, the compact set that we wish to globally asymptotically stabilize is defined as

$$\mathcal{A} := \mathcal{Z}^* \times \mathbb{R}_{\geq 0} \times \mathcal{Q} \times \mathbb{R}_{\geq 0} \subset \mathcal{X}, \quad \text{with} \quad \mathcal{Z}^* = \bigcup_{q \in \mathcal{Q}} \mathcal{Z}_q^*. \tag{55}$$

Condition (L1) is satisfied since $(\overline{C} \cup D \cup G(D)) \subset \mathcal{X}$ and $\text{dom}\, \mathcal{L} = \mathcal{X}$. Similarly, because both $\mathcal{A}$ and $C \cup D \cup G(D)$ are subsets of $\mathcal{X}$, condition (L2) holds. By assumption, for each $q \in \mathcal{Q}$, $\hat{V}_q$ is Lipschitz continuous on $\mathcal{Z}$, which ensures that $\mathcal{L}$ is continuous on $\mathcal{X}$ and locally Lipschitz on an open subset containing $\overline{C} \cap \mathcal{X}$; hence, condition (L3) is satisfied. By assumption, for each $q \in \mathcal{Q}$, the corresponding value function $\hat{V}_q$ attains its global maximum at $\mathcal{Z}_q^*$ and strictly decreases as the distance from $\mathcal{Z}_q^*$ increases. Hence, each value function $\hat{V}_q$ is negative definite with respect to $\mathcal{Z}^*$. Therefore, by construction, for each $q \in \mathcal{Q}$ the Lyapunov function in (54) is positive definite on $\mathcal{X}$, and hence on $C \cup D \cup G(D)$, with respect to $\mathcal{A}$, so that condition (L4) is satisfied.

Next, we use the Lyapunov candidate function in (54) to show that $\mathcal{H}$ globally asymptotically stabilizes $\mathcal{A}$. According to Sanfelice (2021, Theorem 3.19), given sets $\mathcal{U}, \mathcal{A} \subset \mathcal{X}$ and a function $\mathcal{L}\colon \mathcal{X} \to \mathbb{R}$ that defines a Lyapunov candidate on $\mathcal{U}$ with respect to $\mathcal{A}$ for the hybrid closed-loop

system $\mathcal{H} = (C, F, D, G)$ with state $x \in \mathcal{X}$, the set $\mathcal{A}$ is asymptotically stable for $\mathcal{H}$ provided that $\mathcal{A}$ is compact, $\mathcal{H}$ satisfies the hybrid basic conditions, every maximal solution x to $\mathcal{H}$ complete, and the following two conditions hold during flows and jumps:

(L5) $\langle \nabla \mathcal{L}(x), F(x) \cap T_C(x) \rangle < 0$ for all $x \in (C \cap \mathcal{U}) \setminus \mathcal{A}$; and

(L6) $\mathcal{L}(G(x)) - \mathcal{L}(x) < 0$ for all $x \in (D \cap \mathcal{U}) \setminus \mathcal{A}$.

By Proposition 1, the hybrid closed-loop system $\mathcal{H}$ satisfies the hybrid basic conditions under the assumptions. Moreover, by Proposition 2, every maximal solution x to $\mathcal{H}$ is complete.

By assumption, for each $q \in \mathcal{Q}$, the corresponding value function $\hat{V}_q$ attains its global maximum at $\mathcal{Z}_q^*$ and strictly decreases as the distance from $\mathcal{Z}_q^*$ increases. Moreover, since each policy $\pi_q \in \Pi$ globally asymptotically stabilizes $\mathcal{Z}_q^*$, the state z globally asymptotically converges toward $\mathcal{Z}_q^*$ along flows, resulting in a strict increase in $\hat{V}_q(z)$ while q remains constant. Consequently, the Lyapunov candidate function in (54) strictly decreases along flows for all $x \in \mathcal{X} \setminus \mathcal{A}$, thereby satisfying condition (L5).

Furthermore, by definition of the jump set D in (24), jumps occur only when $q \in \mathcal{Q} \setminus Q^*(z)$; the jump map G in (19) then updates q to an element of $Q^*(z)$. Since $\hat{V}_{q'}(z) > \hat{V}_{\bar{q}}(z)$ for all $q' \in Q^*(z)$ and $\bar{q} \in \mathcal{Q} \setminus Q^*(z)$ for each $z \in \mathcal{Z}$, it follows that the Lyapunov candidate function undergoes a strict decrease at jumps, satisfying condition (L6).

As all the conditions above are satisfied, the hybrid closed-loop system $\mathcal{H}$ globally asymptotically stabilizes the compact set $\mathcal{A}$. This, in turn, renders the compact set $\mathcal{Z}^*$ asymptotically stable, and thus condition (P1) is satisfied.

Proposition 2 guarantees that, under its assumptions—that for each $q \in \mathcal{Q}$ the approximate value function $\hat{V}_q \colon \mathcal{Z} \to \mathbb{R}$ is continuous and both the policy $\pi_q \colon \mathcal{Z} \to \mathcal{U}$ and the dynamics $f \colon \mathcal{Z} \times \mathcal{U} \to \mathcal{Z}$ are Lipschitz continuous—every maximal solution to the hybrid closed-loop system $\mathcal{H}$ in (17)-(24) is complete, non-Zeno, and has jump times uniformly lower bounded by a positive constant. Consequently, in the absence of measurement noise, arbitrarily fast switching, that is, chattering, cannot occur.

Now, suppose that measurement noise m satisfying $0 < |m| \leq \varepsilon$ is present such that $z + m \in \mathcal{Z}$. Then, it is possible that a policy q belongs to $Q^*(z)$ while $q \notin Q^*(z+m)$; that is, the optimal policy for the measured state $z + m$ may differ from the optimal policy for the true state z. To prevent an instantaneous switch in such cases, we must ensure that the dwell-time parameter δ_d is always reset to a value greater than zero. Since the jump set (24) requires that $\tau \geq \delta_d$ and the timer τ is reset to zero upon each switch, a positive reset value for δ_d guarantees that a nonzero time interval of at least δ_d must elapse before another jump occurs.

To establish that δ_d is always positive, consider its update in (19). Two scenarios arise:

1. If the set $\mathcal{T}$ is empty, then by definition δ_d is reset to $\bar{\delta}_d > 0$.
2. If $\mathcal{T}$ is non-empty, let η^* denote the smallest time horizon in $\mathcal{T}$, that is, the smallest $\eta^* > 0$ for which the ratio in (20) reaches μ. By the definition of Q^* in (9), for every $z \in \mathcal{Z}$ and every $q \in Q^*(z)$ we have

$$\hat{V}_q(z) \geq \hat{V}_{\bar{q}}(z) \quad \text{for all } \bar{q} \in \mathcal{Q}.$$

In particular, at $\eta = 0$ we obtain

$$\frac{\max\limits_{\bar{q} \in (\mathcal{Q} \setminus \{q\})} \hat{V}_{\bar{q}}\big(\chi(0)\big) - \hat{V}_q\big(\chi(0)\big)}{|\hat{V}_q\big(\chi(0)\big)| + \epsilon} < 0, \tag{56}$$

for all $q \in Q^*(\chi(0))$ and $\chi(0) \in \mathcal{Z}$. Moreover, as demonstrated in the proof of Proposition 1, the ratio in (20) has a continuous dependency on the initial state $\chi(0)$. Therefore, there exists a

smallest time $\eta^* > 0$ such that

$$\frac{\max\limits_{\bar{q}\in(\mathcal{Q}\setminus\{q\})} \hat{V}_{\bar{q}}\big(\chi(\eta^*)\big) - \hat{V}_q\big(\chi(\eta^*)\big)}{|\hat{V}_q\big(\chi(\eta^*)\big)| + \epsilon} = \mu. \tag{57}$$

Since the ratio at $\eta = 0$ is strictly negative and $\eta \in [0, \bar{\delta}_d]$, it follows that $\eta^* > 0$. Consequently, the updated value of δ_d is always positive.

Thus, even in the presence of measurement noise, the requirement $\tau \geq \delta_d > 0$ ensures that a positive dwell time elapses between jumps, thereby preventing arbitrarily fast policy switching. Hence, condition (P2) is satisfied. □